A New Approach for Real-Time Tool Dedicated to The Detection of Broken Bar Fault in Induction Motor

M.A. MOUSSA,Y. MAOUCHE, M.E.K. OUMAAMAR, A. KHEZZAR

Laboratoire d'électrotechnique de Constantine
Département d'électrotechnique
Université Constantine 1, 25000, Constantine, Algeria
Mohamed-Amine.MOUSSA@lec-umc.org

Abstract

The diagnostic methods for electrical motors developed during the last decades based on the FFT and DFT signal-processing algorithms do not have the capability to handle and identify the dynamic changes in the magnitude of the default signature components. The authors in this paper focus on the use of new approach for real-time tool dedicated to the detection of broken bar fault in induction motor, this approach based on sliding DFT window allows the monitoring the broken bar faults using the induced oscillation in the magnitude of the some harmonic components in the stator current. Simulation and experimental results show the effectiveness of the proposed approach.

1. Introduction

The broken bar fault can damage motor performance because it can cause the torque and speed ripple, decrease average torque, noise and unbalance of stator current. Around 5-10% of total induction motor failures are rotor failures and, more specifically, broken rotor bars and end-ring faults [1]. For these reasons, amount of paper has been published dealing with broken bar fault detection [1]-[8]. Most of them are based on use of the most accessible parameter in industry; motor current signature analysis (MCSA) and vibration [2]-[3]. The (MCSA) technique investigates the fault indicative frequencies around fundamental supply frequency or by surveillance the rotor space harmonic components.

Several techniques have been presented in literature to shed light on the presence of characteristic fault frequencies in the stator current, the basic one is based on spectrum computed using FFT or DFT algorithms. However, in on-line monitoring of machine conditions the use of FFT brings an overwhelming burden to the DSP causes by the calculation of the other unneeded frequencies. The use of DFT allows us to avoid this drawback by calculating only the characteristic frequencies components related to faults, but on the other hand, it becomes obsolete when we have to deal with the amplitude oscillation of these components.

The authors in this paper focus on the use of new approach for real-time tool dedicated to the detection of broken bar fault in induction motor, this approach based on sliding DFT window allows the monitoring the broken bar faults using the induced oscillation in the magnitude of some harmonic components in the stator current.

2. DFT sliding windows

The Discrete Fourier Transform DFT $I_s(k)$ of order k of the stator current from N samples can be given by [6]:

$$I_s(k) = \sum_{n=0}^{N-1} i_s(n) W_N^{nk} \tag{1}$$

where:

$$W_N^{nk} = exp(-\frac{j2nk}{N}), k = 0, 1, \cdots, N-1$$

The last N sample are denoted $[i_s(N)]$ and when a new data sample becomes available, the input vector is shifted by one position forward in time, and the new input vector becomes $[i_s(N)]$, where:

$$[i_s(N-1)] = \begin{bmatrix} i_s(0) \\ i_s(1) \\ \vdots \\ i_s(N-k) \\ \vdots \\ i_s(N-1) \end{bmatrix} \quad [i_s(N)] = \begin{bmatrix} i_s(1) \\ i_s(2) \\ \vdots \\ i_s(N-k+1) \\ \vdots \\ i_s(N) \end{bmatrix}$$

By expanding (1) for $[i_s(N-1)]$ noted $I_s(k)_{old}$ and for $[i_s(N)]$ noted $I_s(k)_{new}$:

$$I_s(k)_{old} = \frac{1}{N}\Big(i_s(0) + i_s(1)W_N^k + i_s(1)W_N^{2k} + \cdots + \tag{2}$$
$$+ i_s(N-k)W_N^{(N-k)k} + \cdots + i_s(N-1)W_N^{(N-1)k} \Big)$$

$$I_s(k)_{new} = \frac{1}{N}\Big(i_s(1) + i_s(2)W_N^k + i_s(1)W_N^{2k} + \cdots + \tag{3}$$
$$+ i_s(N-k+1)W_N^{(N-k)k} + \cdots + i_s(N)W_N^{(N-1)k} \Big)$$

Using (2) and (3) we can find the sliding windows formula:

$$I_s(k)_{new} = \Big(I_s(k)_{old} - i_s(0)\Big)W_N^{-k} + i_s(N)W_N^{(N-1)k} \tag{4}$$

This last relation shows how we can save the computation, where the new DFT component is calculated recursively from the previous one (Fig. 1).

The analyzed method in (4) has been implemented using Dspace (DS-1104) to compute a desired components frequencies for real time application.

The prediction of the exact motor slip is necessary to compute only the fault signatures as $(1-2s)f_s$. For that we have to look around the first rotor slot harmonic RSH on the component with the highest magnitude, where:

$$f_{RSH} = f_s \left[\frac{\lambda n_b}{p}(1-s) \pm s \right] \tag{5}$$

then, we get the slip:

$$s = \left[1 - \frac{p}{\lambda n_b} \left(\frac{f_{RSH}}{f_s} - 1 \right) \right] \tag{6}$$

where : $\lambda = 1, 2, 3, ...$, p the motor pole pair number and n_b the rotor bar number.

2.1. Stator current analysis

The broken rotor bars induce in the stator winding additional components at frequencies given by: [8]

$$f_{sbr} = (1 \pm 2ks)\, f_s \tag{7}$$

Fig. 2 shows the magnitude of harmonic $(1-2s)f_s$ calculated by using FFT for different tests under the same conditions (induction motor has one broken bar fault and constant load). One can notice that the magnitude of $(1-2s)f_s$ changes independently of load and fault levels. It is evident that the analyze of the magnitude is not suitable for a precise decision on the rotor conditions, that is due to its fluctuation where the difference can be more than 15dB. For that, considering the fault signature fluctuations would be more than necessary.

3. Simulation study

The simulation analysis was performed on a 24 stator slots 22 bars, 2 pair poles and a rated power of 1.1Kw. The dynamic simulation was carried out using the model developed in [8] and [9]. The SDFT is used in parallel process to simulate the on-line setup and the changes in the stator current spectrum are computed for every step of simulation (Fig. 1). A particular interest is conducted for the fluctuation of the fundamental and $(1-2s)f_s$ components of the stator currents as the most pronounced ones.

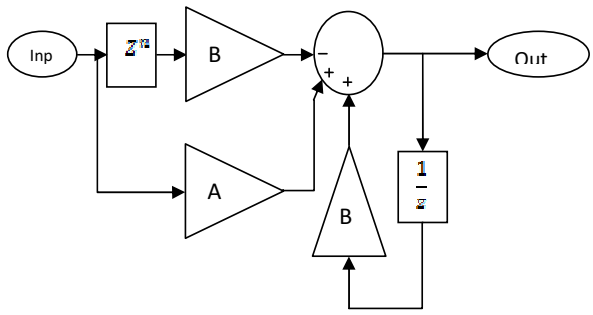

Figure 1. Sliding window structure.

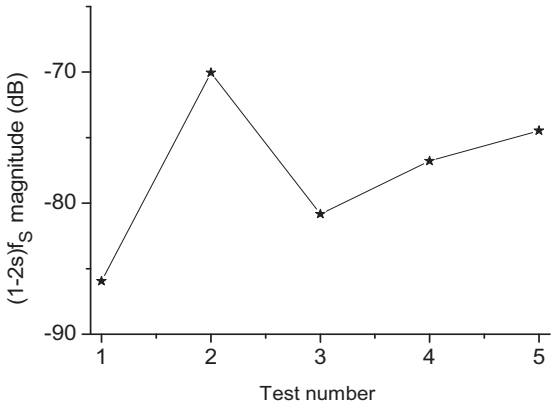

Figure 2. The magnitude of harmonic $(1-2s)f_s$ for different instants and under broken bar fault for the same conditions.

3.1. On-line detection of rotor broken bar based on the fluctuation of the fundamental magnitude of the stator current

Figure 3 shows the magnitude of fundamental component of stator current, for different loads and for healthy conditions. One can see clearly that the magnitude of fundamental harmonic is almost constant in this case, but when the broken bar fault is introduced we notice the fluctuation of this component (Fig. 4). This additional fluctuation does not show up when the motor is not loaded.

Figure 5 shows The FFT of the magnitude of the stator current fundamental component where we can see that the additional pulsation in the case of faulty motor is multiple of $2sf_s$ and be considered as a new broken bar signature.

3.2. On-line detection of rotor broken bar based on the fluctuation of $(1-2s)f_s$ magnitude of the stator current

Figure 6 shows the magnitude of $(1-2s)f_s$ with different load levels, under healthy condition. The magnitudes of $(1-2s)f_s$ for 20%, 40% and 70% of the nominal load are under $-100\ dB$ which means the absence of this component. On the other hand, the magnitude of this component is so significant when the motor is not loaded that because in this case, the $(1-2s)f_s$ component is so close to f_s the fundamental component. For that, the showed value is that of f_s.

Figure 7 illustrates the magnitude of $(1-2s)f_s$ for different load levels and under broken bar fault condition. It is easy to notice the fluctuation of the magnitudes of $(1-2s)f_s$ in this case. We can noticed the same remark as above for the no-loaded case where the fundamental component appears in the place of $(1-2s)f_s$ one.

Fig.8 presents the FFT spectrum of magnitude of $(1-2s)f_s$ for $s = 0.0557$. One can notice under broken bar fault condition, that in plus of the dc component appear the multiple of $2sf_s$ components and they are more pronounced than of those of the fundamental magnitude ones. These components can also considered as original ones for the diagnostic of the rotor conditions.

4. Experimental validation

In order to confirm the simulation results, several experimental evaluations are carried out by using test setup shown in Fig. 9. The induction motor is three-phase 1.1-kW with 24 sta-

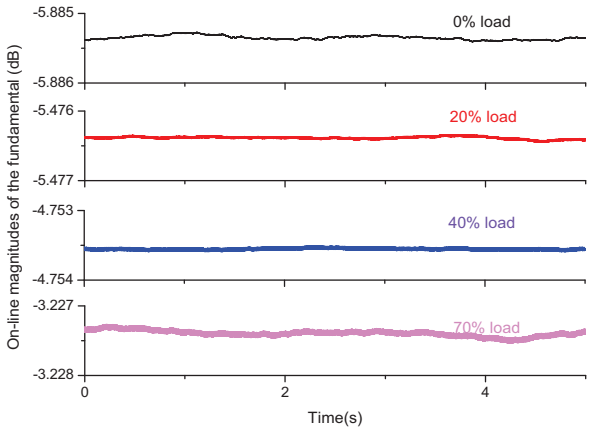

Figure 3. Simulation results. Magnitude of fundamental component of the stator current of a healthy motor. From top to bottom different loads.

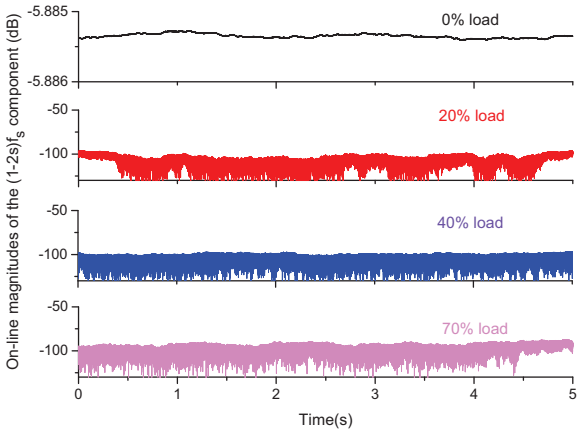

Figure 6. Simulation results. Magnitude of $(1-2s)f_s$ component of the stator current of a healthy motor. From top to bottom different loads.

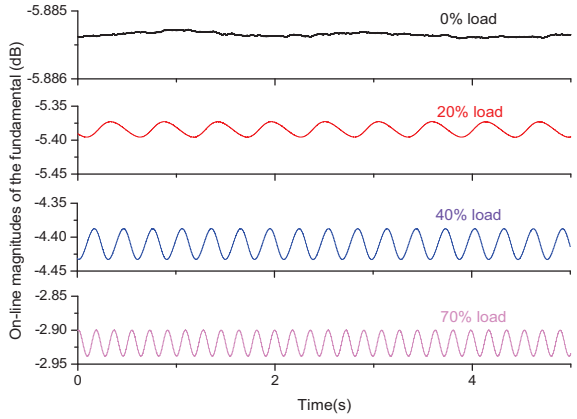

Figure 4. Simulation results. Magnitude of fundamental component of the stator current of a motor with one broken bar. From top to bottom different loads.

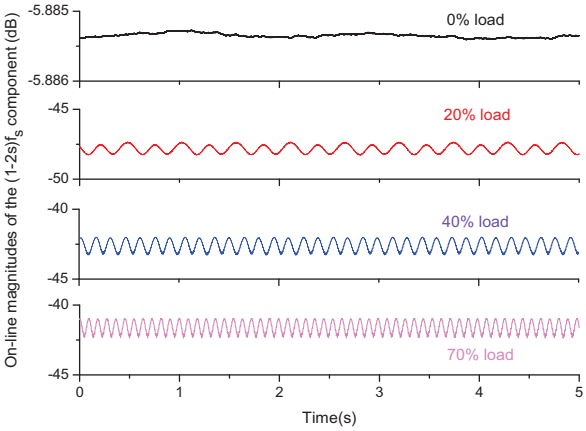

Figure 7. Simulation results. Magnitude of $(1-2s)f_s$ component of the stator current of a motor with one broken bar. From top to bottom different loads.

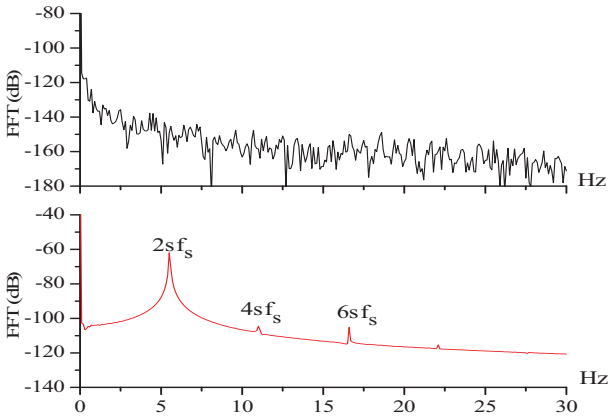

Figure 5. Simulation results. The FFT of the fundamental amplitude of the stator current, $s = 5.5\%$. Top healthy motor and bottom with one broken bar.

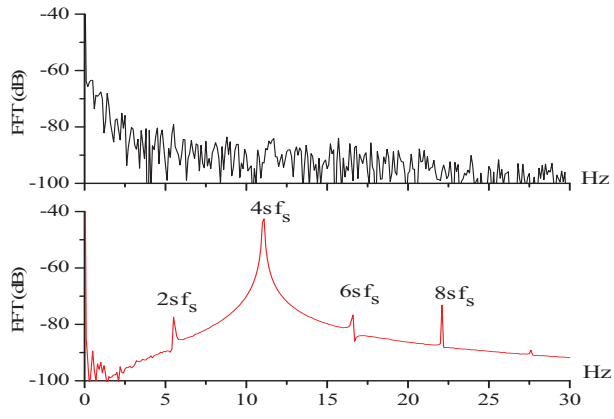

Figure 8. Simulation results. The FFT of the amplitude of $(1-2s)f_s$ of the stator current, $s = 5.5\%$. Top healthy motor and bottom with one broken bar.

tor slots, 22 rotor bars, and 2 pair poles. For the rotor fault, the bar has been broken by drilling it. It was supplied directly from the power line and equipped with current probe. The load is a magnetic powder brake, the stator line current of the motor is processed by DSpace DS1104 board using SDFT algorithm. In the same approach as simulation one, several tests have been made under both healthy and faulty conditions where we have evaluated the rotor conditions by the presence or the vanishing of the fluctuation in the magnitude of the fundamental and $(1-2s)f_s$ components.

Figures 10 and 11 show the on-line amplitude of the fundamental component of the stator current for both cases healthy motor and with broken bar one respectively. The experimental results confirm the presence of broken bar introduces fluctuations on the fundamental component. These fluctuation is well pronounced and even in the case of no-loaded motor. This last remark is so interesting because it is well known that it is so difficult to have a clear broken bar signature for a weak load.

The FFT spectrum of this component is showed on the Fig. 12 where it is clear that the frequency of additional fluctuation caused by the broken bar fault is $2sf_s$ and its multiple components.

Figures 13 and 14 show the on-line amplitude of $(1-2s)f_s$ component of the stator current for both healthy motor and with one broken bar one. In the case of healthy motor we noticed the presence of a weak fluctuation as a signature of constructional fault. for the second case where one broken bar is considered, we notice the clear fluctuation even for the weak load, with multiple of $2sf_s$ frequencies (Fig. 12 and 15).

Figures 16 confirms experimentally that the diagnostic of rotor broken bar is possible even when the motor is not loaded, and the appearance of the $2sf_s$ frequency makes the decision easy.

5. Conclusion

This paper has investigated a new approach for real-time tool dedicated to the detection of broken bar fault in induction motor. The new approach is based on the frequencies oscillation of magnitude of characteristic frequencies related to faulty and healthy conditions of the induction motor. The diagnosis of the broken bar fault can be reliably performed; the method presented in this paper is very suitable for on-line analysis in the present of broken bar and work is in progress for other motor failures.

Figure 9. View of the experimental system.

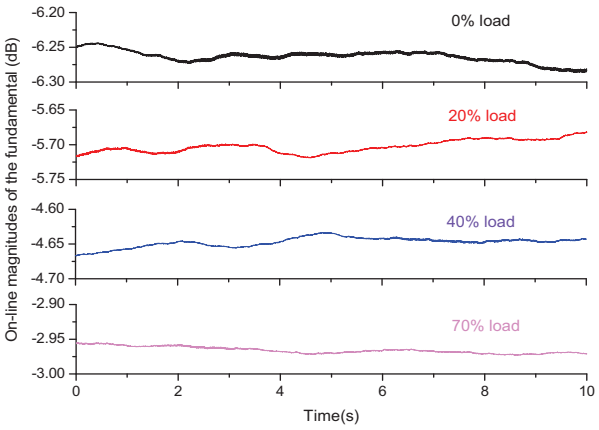

Figure 10. Experimental results. Magnitude of fundamental component of the stator current of a healthy motor. From top to bottom different loads.

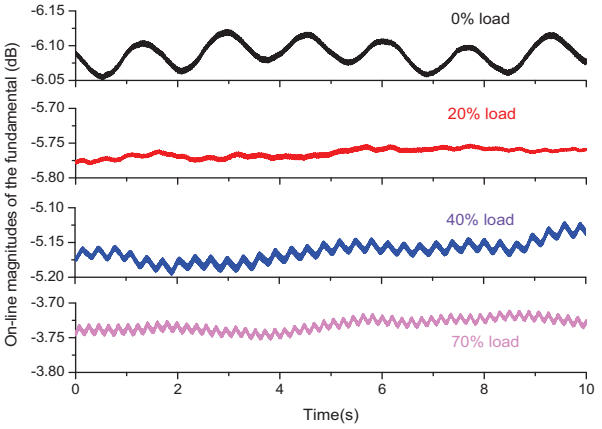

Figure 11. Experimental results. Magnitude of fundamental component of the stator current of a motor with one broken bar. From top to bottom different loads.

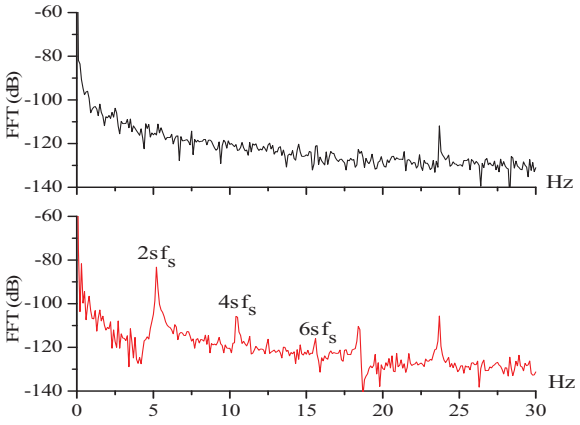

Figure 12. Experimental results. The FFT of the fundamental amplitude of the stator current, $s = 5.2\%$. Top healthy motor and bottom with one broken bar.

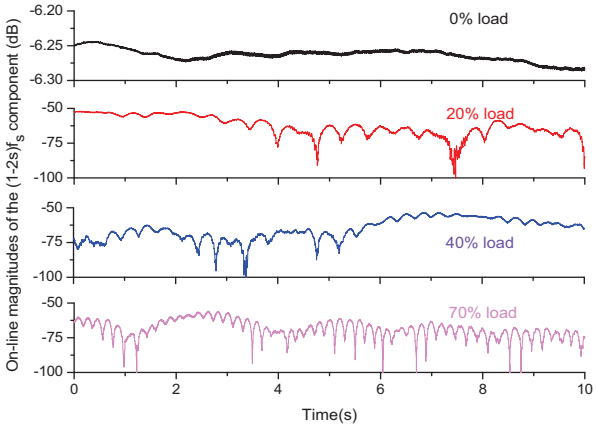

Figure 13. Experimental results. Magnitude of $(1-2s)f_s$ component of the stator current of a healthy motor. From top to bottom different loads.

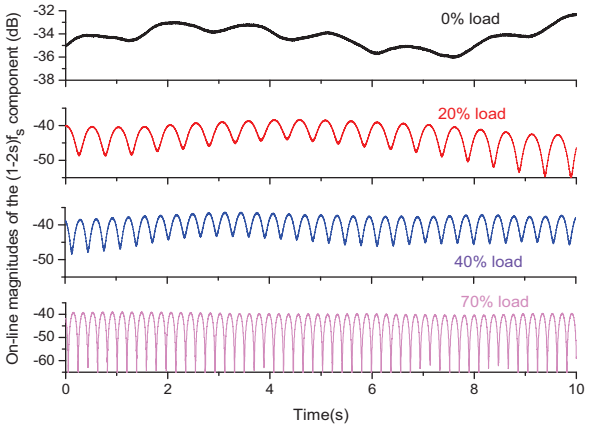

Figure 14. Experimental results. Magnitude of $(1-2s)f_s$ component of the stator current of of a motor with one broken bar. From top to bottom different loads.

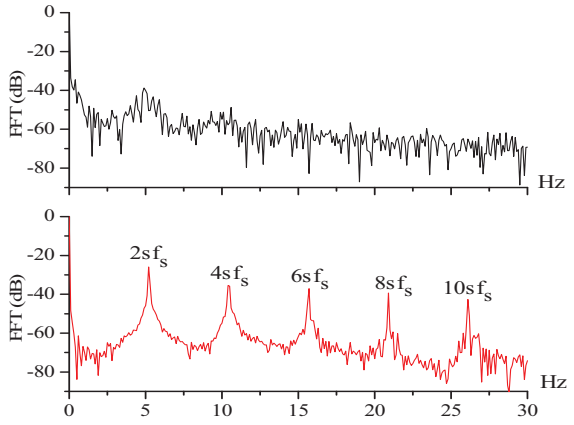

Figure 15. Experimental results. The FFT of the amplitude of $(1-2s)f_s$ of the stator current, $s = 5.2\%$. Top healthy motor and bottom with one broken bar.

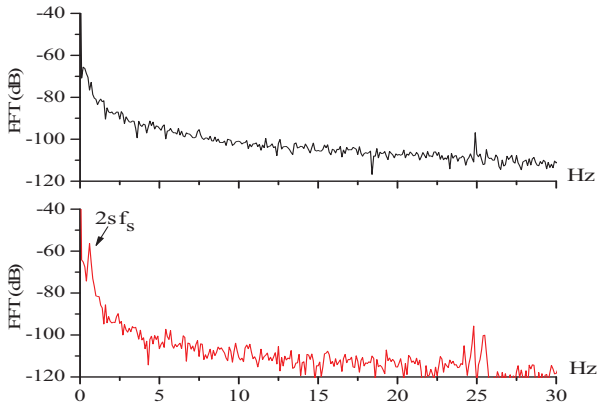

Figure 16. Experimental results. The FFT of the fundamental amplitude of the stator current, motor no loaded. Top healthy motor and bottom with one broken bar.

6. References

[1] A. Bellini, C. Concari, G. Franceschini, C. Tassoni, and A. Toscani, "Vibrations, currents and stray flux signals to asses induction motors rotor conditions", in Proc. IECON, pp: 4963-4968, Nov. 2006.

[2] J.-H. Jung, J.-J. Lee, and B.-H. Kwon, "Online diagnosis of induction motors using MCSA", IEEE Trans. Ind. Electron., vol. 53, no. 6, pp: 1842-1852, Dec. 2006.

[3] Concari C, Franceschini G, Tassoni C. "Differential diagnosis based onmultivariable monitoring to assess induction machine rotor conditions", IEEETrans Ind Electron, vol. 55, no. 12, pp:4156-4166, Dec. 2008.

[4] Yeh CC, Povinelli RJ, Mirafzal B, Demerdash NAO. "Diagnosis of stator winding inter-turn shorts in induction motors fed by PWM-Inverter drive systems using a time-series data mining technique.", In: Proceedings of IEEE international conference on power system technology, vol. 1, pp: 891-896, Singapore, Nov. 21-24. 2004

[5] P. Vaclavek and P. Blaha, "Speed estimation scheme for small AC induction machine sensorless control", in Proc. 33rd IEEE IECON, pp: 986-991, Nov. 5-8 2007.

[6] Patrice Nus, Traitement numerique du signal, Publitronic-Elektor, 1998. ISBN: 2-86661-091-1

[7] A. Abed, F. Weinachter, H. Razik, and A. Rezzoug, "Real-time implementation of the sliding DFT applied to on-line broken bars diagnostic",in Proc. IEEE IEMDC, 2001, pp. 345-348.

[8] A. Khezzar, M.E.K. Oumaamar,M. Hadjami, M. Boucherma and H. Razik, "Induction Motor Diagnosis Using Line Neutral Voltage Signatures",Industrial Electronics, IEEE Transactions on, vol. 56, no: 11, pp: 345-348, 2009.

[9] A. Khezzar,M. Hadjami, N. Bessous M.E.K. Oumaamar and H. Razik, "Accurate modelling of cage induction machine with analytical evaluation of inductances",Industrial Electronics, 2008. IECON 2008. 34th Annual Conference of IEEE, pp: 1112-1117, 10-13 Nov. 2008.